Received: 20 September 2020 | Revised: 13 November 2020 | Accepted: 4 December 2020

IET Renewable Power Generation

DOI: 10.1049/rpg2.12045

The Institution of Engineering and Technology WILEY

ORIGINAL RESEARCH PAPER

Optimal day-ahead scheduling for active distribution network based on improved information gap decision theory

Xiaolin Ge[1] | Xiaohe Zhu[1] | Xing Ju[2] | Yang Fu[1] | Kwok Lun Lo[3] | Yang Mi[1]

[1] College of Electrical Engineering, Shanghai University of Electric Power, Shanghai, People's Republic of China

[2] Beibei Electricity Supply Company, State Grid Chongqing Municipal Electric Power Company, Chongqing, People's Republic of China

[3] Department of Electronic and Electrical Engineering, University of Strathclyde, Glasgow, UK

Correspondence
Yang Fu, College of Electrical Engineering, Shanghai University of Electric Power, Shanghai, People's Republic of China.
Email: mfudong@126.com

Funding information
National Natural Science Foundation of China, Grant/Award Number: 52077130; Shanghai Engineering Research Center of Green Energy Grid-Connected Technology, Grant/Award Number: 13DZ2251900; Shanghai Science and Technology Project, Grant/Award Number: 18DZ1203200

Abstract

In this study, information gap decision theory (IGDT) is reformed to formulate the uncertain parameters of wind power, photovoltaic and load. Traditional IGDT presumes that positive and negative deviations of uncertain parameters of the predicted value are equal, and it would result in imprecise assessment of fluctuated intervals. This study proposes an improved IGDT to overcome the inaccuracy of traditional IGDT by considering unsymmetrical fluctuation levels of uncertainties. For the operation and control of active distribution network, the non-linear power flow constraints are included and linearised with a novel method based on circumscribed polyhedron approximation, which guarantees the accuracy of the solution results and takes less computing time. Additionally, from the mathematical point of view, the model established in this study is a multilevel optimisation problem, and linear Karush–Kuhn–Tucker conditions are formulated to transform the multilevel optimisation problem into a single-level optimisation problem. Finally, the economic viability and model applicability are verified through the modified IEEE 33-node distribution system.

1 | INTRODUCTION

As different types of distributed generations (DGs) have been integrated into the power network in recent years, the distribution network is changing gradually from a traditional passive system to a modern active one on its operation and management. Thus the concept of active distribution network (ADN) has been put forward, and some practical research results have been achieved [1]. Considering that the power output of DGs and the demand of loads are difficult to predict accurately, and the power exchange between ADN and the bulk power system is bidirectional, the optimised operation of ADN is very challenging. Recently, it has been widely concerned how to take into account the uncertainty of DGs and the demand of loads in the research of optimal dispatching of ADN [2–4].

Several approaches have been developed to improve ADN operational adequacy with the consideration of uncertainty. The probabilistic optimal power flow model can be presented to cope with wind power integration [5, 6]. A chance constrained framework is established in [7, 8] to address the security problem caused by the uncertainties of DGs. A grey-box model is proposed in [9] to deal with the uncertainty of photovoltaic (PV) power. In [10], the probabilistic locational marginal price is employed to deal with the forecasting error of load. However, the mentioned studies only consider either the uncertain power output of DGs or the uncertain demand of load but neglect the combined influence of these two aspects on the operation of the distribution network. The uncertainties of multiple DGs and load are considered in [11, 12] with robust and multi-scene optimisation methods. However, multi-scene optimisation method

TABLE 1 Comparison between the existing and the proposed methods

No.	Source of methods	Object	Uncertainty modelling	Demand for uncertain information	Positive and negative deviations of uncertain information	Solving method
1	[11]	Uncertainty of wind	Multi-scene	Much	Unsymmetrical	Bucket
2	[12]	Uncertainties of DGs and load	Robust	Much	Unsymmetrical	column-and-constraint generation
3	[14]	Uncertainty of wind	Information gap decision theory (IGDT)	Less	Symmetrical	Mixed integer non-linear programming
4	[16]	Uncertainty of electricity market price	IGDT	Less	Symmetrical	Boundary value
5	[19]	Uncertainty of reactive power balance	Gauss-type and *Z*-type	Much	Unsymmetrical	Intelligent algorithms
6	Proposed	Uncertainties of distributed generations and load	Improved IGDT	Less	Unsymmetrical	Mixed integer linear programming (MILP)/ Karush–Kuhn–Tucker

is dependent on the probability statistics data; in fact, it is difficult to obtain the accurate statistical data of DGs power and load. Robust optimisation method is used to ensure the feasibility of all possible scenarios, and thus leads to conservative results.

To make decision with less information of uncertain parameters and guarantee the economy of system operation, the information gap decision theory (IGDT) is developed in [13]. A non-probabilistic information gap model is used in [14] to formulate the uncertainties in short-term scheduling of energy hub system, which is independent of historical data and can guarantee the net cost of energy hub scheduling lower than expected. In [15], IGDT is proposed as a basic approach for enhancing decision making under uncertainty, especially when less information is available. However, the traditional IGDT method assumes that positive and negative deviations of uncertain parameters from the predicted value are equal, which would result in the fluctuated intervals being assessed inaccurately. Therefore, a more accurate model is needed to overcome the disadvantage of traditional IGDT.

The boundary value method is used to solve the IGDT model, which tests the feasibility of solutions in typical scenarios and simplifies the calculation, but the method might cause the solution to be too optimistic [16, 17]. In fact, the IGDT-based model in this study is a multilevel optimisation problem. Karush–Kuhn–Tucker (KKT) conditions can be used as an effective method to transform multilevel optimisation problem into an equivalent single-level optimisation problem [18]. However, solving the problem can become more difficult with non-linear KKT conditions. So, the intention of this study is to overcome this obstacle, and build efficient KKT conditions to solve the optimal scheduling problem of ADN.

In ADN systems, various types of DGs are connected, and corresponding non-linear constraints are included in the model of optimal scheduling of ADN. In recent years, some improved intelligent algorithms [19, 20] have been employed to solve the mixed integer non-linear programming (MINLP) model directly, but they still cannot always give a proper balance between computational time and the accuracy of the solution results. Second-order cone programming (SOCP) is a convex programming method and can improve the solution efficiency of non-linear model with high accuracy [21]. However, it remains to be solved on how to transform SOCP into a mixed integer linear programming (MILP).

In this context, an optimal scheduling model of ADN based on an improved IGDT is established in this study and is transformed into a MILP model with a new cone linearisation method based on circumscribed polyhedron approximation (CPA), which reduces the solving difficulty of optimal scheduling model of ADN. In addition, linear KKT conditions are established to convert the multilevel optimisation problem into an equivalent single-level optimisation problem. Finally, a modified IEEE 33-node power distributed system is used to validate the performance of the proposed improved model and method of solution.

The comparison between typical existing works and the proposed approach is reported in Table 1. Compared with the uncertainty modelling methods presented in [11, 12, 19], IGDT does not rely on historical data, requires less uncertain information, and ensures strong decision-making ability. Meanwhile, different from the existing IGDT method, this study considers that the fluctuation range of positive and negative deviations between the uncertain parameters and the predicted values are unsymmetrical, which makes the estimation of the fluctuated intervals more accurate. Other features of the proposed approach include transforming the ADN model into an easily solved MILP model with CPA and linear KKT conditions.

The main contributions of this study are as follows:

1. An improved IGDT model is developed to obtain accurate assessments of fluctuated intervals of uncertain parameters, and it takes into consideration the different amplitudes of positive and negative deviations of uncertain parameters from the predicted values. Correspondingly, a new objective

function that can describe the relationship between the cost and uncertain parameters is formulated in this study.
2. Complex non-linear constraints are included in the established ADN model, such as the power flow constraints and branch power limits, and converted into an MILP model by a new cone linearisation method with CPA. The CPA method not only reduces the difficulty of solving the model but also improves the speed of calculation.
3. To evaluate the maximum and minimum cost of the system simultaneously, two sets of KKT conditions are subtly designed for the IGDT model, and the multilevel optimisation problem is converted into a single-level optimisation equivalent problem. In addition, the KKT conditions are converted to mixed integer linear constraints, which is beneficial to the improvement of computational efficiency.

2 | AN IMPROVED MODEL CONSIDERING THE UNCERTAINTIES OF WIND POWER, PV AND LOAD

2.1 | Total day-ahead operation costs of ADN systems

The total cost of the operation of ADN in the day-ahead scheduling horizon can be expressed as

$$C = \sum_{t=1}^{T} \left\{ \sum_{g=1}^{N_g} C_{g}^{t} P_{g}^{t} + \sum_{d=1}^{N_d} (a_d {Pd_d^t}^2 + b_d Pd_d^t + c_d) \right. \tag{1}$$

$$\left. + \sum_{k=1}^{N_k} Ck_k^t Pk_k^t - \sum_{g=1}^{N_g} Cs_g^t Ps_g^t \right\} \Delta T \tag{1}$$

Equation (1) reveals that the total cost contains the purchased costs from the upper grid, generation cost of micro-turbine, and the managed costs of the demand side, except for profits of the power sold to the upper grid. The generation cost function $a_d {Pd_d^t}^2 + b_d Pd_d^t + c_d$ of micro-turbine can be linearised with piecewise linearisation method [22].

2.2 | Objective function based on the improved IGDT

In the actual optimal scheduling problem, the power output of wind turbine, PV and the demand of load are uncertain and the forecasting information is limited; so in this study, it assumes that only the predicted value can be obtained. To describe the uncertainty, the traditional IGDT model presented in [14] formulates equal positive and negative deviations of uncertain parameters from the predicted value, which will result in an imprecise assessment of fluctuated intervals. To overcome the inaccuracy of traditional IGDT, an improved IGDT model is proposed in this study with different fluctuation levels of uncertainties, and the detailed formulations are as follows:

$$(1 - Z_{wa}) Pwr_w^t \le Pw_w^t \le (1 + Z_{wb}) Pwr_w^t \tag{2}$$

$$(1 - Z_{va}) Pvr_v^t \le Pv_v^t \le (1 + Z_{vb}) Pvr_v^t \tag{3}$$

$$(1 - Z_{la}) Plr_l^t \le Pl_l^t \le (1 + Z_{lb}) Plr_l^t \tag{4}$$

Expressions (2)–(4) represent the active power output of wind, PV and load fluctuate in a certain range of the predicted value. Z_{wa}, Z_{wb}, Z_{va}, and Z_{vb}, Z_{la}, Z_{lb} are positive and negative deviations of uncertain parameters of wind, PV and load, respectively, from the corresponding predicted values.

In order to make the maximum and minimum operation cost of the system within the expected value, limits of generation cost functions are built:

$$\max C \le C_{cb}, C_{cb} = (1 + \delta_{cb}) C_o \tag{5}$$

$$\min C \le C_{co}, C_{co} = (1 - \delta_{co}) C_o. \tag{6}$$

Equations (5) and (6) indicate that the constraints of the maximum and minimum generation cost of and, respectively, and they will not exceed the expectations.

As the system cost decreases with the increase of wind and PV output and the reduction of load demand, a new multi-objective function is established to satisfy Equations (5) and (6) as follows:

$$\max Z_{wa},\ \max Z_{va},\ \max Z_{lb}\ \max -Z_{wb}\ \max -Z_{vb}\ \max -Z_{la} \tag{7}$$

Since the multi-objective functions are modelled as the maximum value of Expression (7), the economic scheduling scheme of ADN realises immunity against the unfavourable deviations of the uncertain parameters.

2.3 | Constraints

The multi-objective functions in Expression (7) should be subject to the following constraints

$$P_i^t = \sum_{j \in \Omega_i}^{n} V_i^t V_j^t (G_{ij} \cos \theta_{ij}^t + B_{ij} \sin \theta_{ij}^t) \tag{8}$$

$$Q_i^t = \sum_{j \in \Omega_i}^{n} V_i^t V_j^t (G_{ij} \sin \theta_{ij}^t - B_{ij} \cos \theta_{ij}^t) \tag{9}$$

$$\sum_{g} (Pg_g^t - Ps_g^t) = \sum_{l} Pl_l^t - \sum_{m_1} Pdg_{m_1}^t - \sum_{k} Pk_k^t \tag{10}$$

$$\sum_{g} (Qg_g^t - Qs_g^t) = \sum_{l} Ql_l^t - \sum_{m_1} Qdg_{m_1}^t - \sum_{k} Qk_k^t \tag{11}$$

$$V_{i,\min} \le V_i^t \le V_{i,\max} \tag{12}$$

$$Pdg_{m_1,\min} \le Pdg^t_{m_1} \le Pdg_{m_1,\max} \tag{13}$$

$$Qdg_{m_1,\min} \le Qdg^t_{m_1} \le Qdg_{m_{1\}},\max} \tag{14}$$

$$S^t_{ij} = \sqrt{\left(P^t_{ij}\right)^2 + \left(Q^t_{ij}\right)^2} \le S_{ij,\max} \tag{15}$$

$$Pk^t_{k,\min} \le Pk^t_k \le Pk^t_{k,\max} \tag{16}$$

$$0 \le P^t_g \le d_1 P^t_{g,\max} \tag{17}$$

$$0 \le P^t_g \le d_2 P^t_{g,\max} \tag{18}$$

$$d_1 + d_2 = 1. \tag{19}$$

Expressions (8)–(11) are power flow constraints, where m_1 is the indices of DGs (including micro-turbines, wind turbines, and PV power stations); Equation (12) represents bus voltage limits; Expressions (13) and (14) are power output constraints of DGs; Equation (15) represents branch power limits; Expression (16) is the interruptible loads limit; and Expressions (17)–(19) represent the constraints of the exchange of power between the feeder and the grid. If feeder sells electricity to the grid, $d_1 = 1$, $d_2 = 0$; otherwise $d_1 = 0$, $d_2 = 1$.

In Models (8)–(19), complex non-linear constraints are included, such as power flow constraints in Equations (8) and (9) and branch power limits in Equation (15); and in addition, binary variables are included in Expressions (17)–(19). Therefore, the proposed improved model is an MINLP model.

3 | CONVERSION OF THE NON-LINEAR FORMULATIONS FOR THE PROPOSED IMPROVED MODEL

As mentioned in Section 2.3, the proposed improved model is an MINLP model and is difficult to solve directly. Thus, the model is transformed into an MILP model, which is easy for the optimisation of the ADN.

3.1 | Linearisation of power flow constraints and branch power limits

To transform power flow constraints in Equations (8) and (9) to a linear function, ancillary variables R^t_i, R^t_j, M^t_{ij}, Z^t_{ij} are introduced as follows:

$$R^t_i = \frac{\left(V^t_i\right)^2}{\sqrt{2}} \tag{20}$$

$$R^t_j = \frac{\left(V^t_j\right)^2}{\sqrt{2}} \tag{21}$$

$$M^t_{ij} = V^t_i V^t_j \cos\theta^t_{ij} \tag{22}$$

$$Z^t_{ij} = V^t_i V^t_j \sin\theta^t_{ij}. \tag{23}$$

The power flow constraints are converted into the following functions:

$$P^t_i = \sum_{j\in\Omega_i}^{n} \left(G_{ij}M^t_{ij} + B_{ij}Z^t_{ij}\right) \tag{24}$$

$$Q^t_i = \sum_{j\in\Omega_i}^{n} \left(G_{ij}Z^t_{ij} - B_{ij}M^t_{ij}\right) \tag{25}$$

$$\left(M^t_{ij}\right)^2 + \left(Z^t_{ij}\right)^2 = 2R^t_i R^t_j \tag{26}$$

Since Equation (26) is difficult to solve, it is converted into

$$\left(M^t_{ij}\right)^2 + \left(Z^t_{ij}\right)^2 + \left(\frac{R^t_i - R^t_j}{\sqrt{2}}\right)^2 = \left(\frac{R^t_i + R^t_j}{\sqrt{2}}\right)^2 \tag{27}$$

And further, Equation (27) is relaxed into a second-order cone.

$$(1-\rho)\frac{R^t_i + R^t_j}{\sqrt{2}} \le \sqrt{\left(M^t_{ij}\right)^2 + \left(Z^t_{ij}\right)^2 + \left(\frac{R^t_i - R^t_j}{\sqrt{2}}\right)^2} \le \frac{R^t_i + R^t_j}{\sqrt{2}} \tag{28}$$

where the value of ρ is small and taken as 10^{-2}.

It is observed that the cone constraints (15) and (28), corresponding to power flow constraints, can be expressed in the form

$$\sqrt{\beta_2^2 + \beta_3^2 + \cdots + \beta_n^2} \le \beta_1 \tag{29}$$

Together with the model in Section 2, the constructed model is a mixed integer SOCP (MISOCP) model.

Such models are used to be solved by MISOCP approach directly [21]. However, it is computationally time-consuming. In order to improve the efficiency of calculation, a new cone linearisation method based on CPA is proposed, which can transform Expression (28) into linearisation formulas.

The proposed cone linearisation method in this study is as follows.

For the cone constraints with three variables in the form

$$\sqrt{\beta_2^2 + \beta_3^2} \le \beta_1, \tag{30}$$

it can be represented as a circular cone and can be obtained by rotating the curve in Equation (31) around the

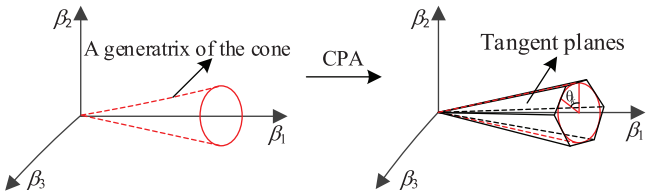

FIGURE 1 The schematic of circumscribed polyhedron approximation (CPA) method in three-dimension coordinate

β_1-axis.

$$\begin{cases} \beta_1 - \beta_2 = 0 \\ \beta_3 = 0 \end{cases} \tag{31}$$

To linearise the cone, a generatrix in Equation (31) is taken from the circular cone. The direction vector is (1, 1, 0), and according to [23], the tangent plane equation of the generatrix is $\beta_1 - \beta_2 = 0$. Therefore, the half-space including the cone is $\beta_1 - \beta_2 \geq 0$.

If the generatrix in Equation (31) rotates anticlockwise around the β_1-axis with angle θ, the direction vector can be obtained as (1, cosθ, sinθ). The corresponding generatrix is expressed as

$$\frac{\beta_1}{1} = \frac{\beta_2}{\cos\theta} = \frac{\beta_3}{\sin\theta} \tag{32}$$

Accordingly, the tangent plane equation can be formulated as

$$\beta_1 - \beta_2 \cos\theta - \beta_3 \sin\theta = 0 \tag{33}$$

And the half-space including the cone is

$$\beta_1 - \beta_2 \cos\theta - \beta_3 \sin\theta \geq 0 \tag{34}$$

It can be found that when rotating with the angle

$$\theta_k = \frac{2k\pi}{q}, \quad k = 1, 2, \ldots, q \tag{35}$$

where q is the total rotating times, the original second-order cone can be approximately represented by the polyhedron that is enclosed with tangent planes as shown in Figure 1 and refers to CPA.

Therefore, the cone in Expression (30) can be substituted by a circumscribed polyhedron with q surfaces as follows:

$$\beta_1 - \beta_2 \cos\frac{2k\pi}{q} - \beta_3 \sin\frac{2k\pi}{q} \geq 0, \quad k = 1, 2, \ldots, q \tag{36}$$

Similarly, for n-dimensional second-order cone in Expression (29), the direction vector at any point can be derived as follows

$$(1, \quad \cos\theta_1 \cos\theta_2 \cdots \cos\theta_{n-2}, \ldots, \cos\theta_1 \cos\theta_2 \cdots \cos\theta_{n-i} \sin\theta_{n-i+1}, \ldots, \sin\theta_1), \quad i = 3, 4, \ldots n \tag{37}$$

where $\theta_1, \theta_2, \ldots, \theta_{n-2}$ are the angles of counterclockwise rotating around each coordinate axis.

Accordingly, the corresponding tangent hyperplane equation passing can be formulated as Equation (38) with the half-space of the cone in Expression (39).

$$\beta_1 - \beta_2 \cos\theta_1 \cos\theta_2 \cdots \cos\theta_{n-2} - \ldots - \beta_i \cos\theta_1 \cos\theta_2 \cdots \cos\theta_{n-i} \sin\theta_{n-i+1} - \ldots - \beta_n \sin\theta_1 = 0 \tag{38}$$

$$\beta_1 - \beta_2 \cos\theta_1 \cos\theta_2 \cdots \cos\theta_{n-2} - \ldots - \beta_i \cos\theta_1 \cos\theta_2 \cdots \cos\theta_{n-i} \sin\theta_{n-i+1} - \ldots - \beta_n \sin\theta_1 \geq 0 \tag{39}$$

Thus, when the angles of counterclockwise rotating around each coordinate axis are set to $2k_j\pi/q_j$, the original n-dimensional second-order cone is linearised with

$$\begin{aligned} &\beta_1 - \beta_2 \cos\frac{2k_1\pi}{q_1} \cos\frac{2k_2\pi}{q_2} \cdots \cos\frac{2k_{n-2}\pi}{q_{n-2}} - \ldots \\ &-\beta_i \cos\frac{2k_1\pi}{q_1} \cos\frac{2k_2\pi}{q_2} \cdots \cos\frac{2k_{n-i}\pi}{q_{n-i}} \sin\frac{2k_{n-i+1}\pi}{q_{n-i+1}} \\ &- \ldots - \beta_n \sin\frac{2k_1\pi}{q_1} \geq 0, k_j = 1, 2, \ldots q_j, j = 1, 2, \ldots n-2 \end{aligned} \tag{40}$$

The preceding derivation process shows that the cone in Equation (15) and Expression (28) related to power flow constraint can be approximated by the CPA method, and taking the right part of Expression (28) as an example, it can be substituted by the following linear constraints:

$$\frac{R_i^t + R_j^t}{\sqrt{2}} - M_{ij}^t \cos\frac{2k_1\pi}{q_1} \cos\frac{2k_2\pi}{q_2} - Z_{ij}^t cos\frac{2k_1\pi}{q_1} \sin\frac{2k_2\pi}{q_2} - \frac{R_i^t - R_j^t}{\sqrt{2}} \sin\frac{2k_1\pi}{q_1} \geq 0 \tag{41}$$

where $q_1 = q_2 = 6$ in this study, and $k_1 = k_2 = 1,2,3,4,5,6$.

The left part of Expression (28) and branch power limits of Expression (15) can also be conversed similarly. Due to space limitation, details of conversion are not included here.

3.2 | The solving of multilevel optimisation problem with KKT conditions

For the convenience of description, the proposed improved model is converted to the form shown in Figure 2.

In Figure 2, $\mathbf{y}$ represents the vector of Z_{wa}, Z_{wb}, Z_{va}, Z_{vb}, Z_{la}, Z_{lb}; $\mathbf{y}^*$ represents the vector of optimum value of $\mathbf{y}$; $\mathbf{x_1}$ and $\mathbf{x_2}$ represent the vector of the other variables corresponding to the maximise and minimise operating cost of and, respectively; and $\mathbf{x_1}^*$ and $\mathbf{x_2}^*$ represent the optimal solution of $\mathbf{x_1}$ and $\mathbf{x_2}$; max $f(\mathbf{y})$ is the objective function in Expression (7). And $\mathbf{g_1}(\mathbf{x_1}^*, \mathbf{y}) \leq 0$ and $\mathbf{g_1}(\mathbf{x_2}^*, \mathbf{y}) \leq 0$ represent constraints in Expressions (2) to (4); $\mathbf{g}(\mathbf{x_1}) \leq 0$ and $\mathbf{g}(\mathbf{x_2}) \leq 0$ represent inequality constraints from Expressions (12) to (18), and (41); and constraint $\mathbf{h}(\mathbf{x_1}) = 0$ and

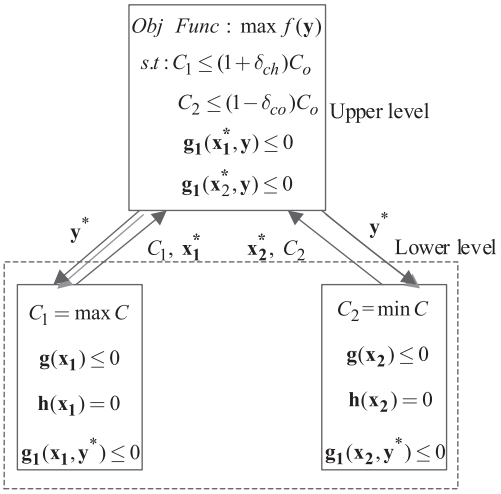

FIGURE 2 The description of the proposed improved model

$\mathbf{h}(\mathbf{x_2}) = 0$ are equality constraint of Expressions (1), (10), (11), (19), (24) and (25).

In previous studies, the boundary value method [16] has been used to solve the multilevel optimisation problem. However, this method has only been tested with some typical scenarios and cannot reliably guarantee the feasibility of the solution. The KKT condition is an effective method for multilevel optimisation problems, which can simplify the original problem and realise equivalent transformation. And thus, two sets of KKT conditions are subtly constructed for IGDT model in this study, and the maximum and minimum costs of the system are evaluated.

1. In order to obtain the maximum operating cost of ADN, the Lagrangian function is formulated as

$$C_1 = L(\mathbf{x_1}, \lambda_1, \mu_1) = C(\mathbf{x_1}) - \sum \lambda_1 \mathbf{g}(\mathbf{x_1}) - \sum \mu_1 \mathbf{h}(\mathbf{x_1}) \tag{42}$$

The KKT conditions for the maximum operating cost of ADN are:

$$\frac{\partial L(\mathbf{x_1}, \lambda_1, \mu_1)}{\partial \mathbf{x_1}} = \frac{\partial C(\mathbf{x_1})}{\partial \mathbf{x_1}} - \lambda_1 \sum \frac{\partial \mathbf{g}(\mathbf{x_1})}{\partial \mathbf{x_1}} - \mu_1 \sum \frac{\partial \mathbf{h}(\mathbf{x_1})}{\partial \mathbf{x_1}} = 0 \tag{43}$$

$$\mathbf{g}(\mathbf{x_1}) \le 0 \tag{44}$$

$$\mathbf{h}(\mathbf{x_1}) = 0 \tag{45}$$

$$\lambda_1 \mathbf{g}(\mathbf{x_1}) = 0 \tag{46}$$

$$\check{}_1 \ge 0. \tag{47}$$

where $\boldsymbol{\mu_1}$ is the vector of Lagrange multiplier for the equality constraints; and $\boldsymbol{\lambda_1}$ is the vector of Lagrange multiplier for the inequality constraints.

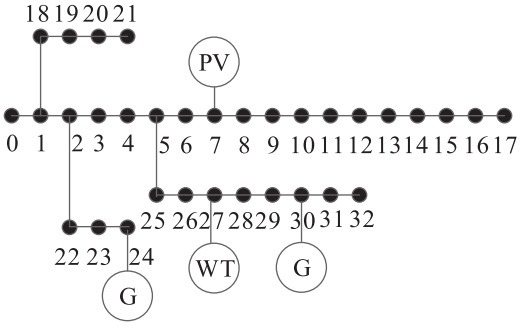

FIGURE 3 Network structure of modified IEEE 33-node distribution system

Equation (46) is a non-linear quadratic constraint and is a combination of Expressions (44) and (47); and when $\boldsymbol{\lambda_1} > 0$, $\mathbf{g(x_1)} = 0$; and when $\boldsymbol{\lambda_1} = 0$, $\mathbf{g(x_1)} \le 0$. Consequently, Equation (46) can be converted to the following linear constraints

$$-\sigma\xi \le \mathbf{g}(\mathbf{x_1}) \le 0 \tag{48}$$

$$0 \le \lambda_1 \le \sigma(1 - \xi) \tag{49}$$

where σ is a large positive number, which can be set to 10^{10}; ξ is a binary variable; and when $\boldsymbol{\lambda_1} > 0$, $\xi = 0$; else $\xi = 1$.

1. To calculate the minimum operating cost of ADN, the corresponding Lagrangian function and KKT conditions can also be constructed similarly and are not discussed in detail due to space limitation.

In conclusion, the optimal scheduling problem of ADN is formulated into a multi-objective MINLP model with the improved IGDT. And then the non-linear power flow and branch power limits are linearised by the proposed CPA. In addition, linear KKT conditions are established to calculate the maximum and minimum costs of the system. Finally, the proposed model is transformed into a multi-objective MILP. The normalised normal constraint method [24] is used to combine the multi-objective function into a single-objective function for optimisation.

4 | CASE STUDIES

4.1 | System parameters

The proposed improved model is solved with CPLEX solver under general algebraic modelling system [25]. The modified IEEE 33-node distribution system [26], shown in Figure 3, is selected to verify the rationality of the proposed method. All tests are carried out on a dual-processor Intel Core i5-6200U with 2.30 GHz CPU and 8.0 GB of RAM.

In the modified IEEE 33-node system, four power sources are added, including two microturbines, one wind turbine, and

TABLE 2 The optimised results of day-ahead scheduling in active distribution network system

Model	Total cost/$	# of constraints	# of variables	Time/s
Mixed integer second-order cone programming [21]	9956.31	81,904	78,973	522.383
MILP with ε-relaxation [30]	9965.76	97,731	92,227	12.454
MILP with circumscribed polyhedron approximation	9959.89	85,914	81,267	8.778

one PV. The accessed points of two microturbines are node 24 and node 30, respectively, and the total installed capacity of the two microturbines is 1 MW. The accessed point of the wind turbine is node 27 and the total installed capacity is 1 MW. The accessed point of the PV power station is node 7 whose total installed capacity is 1 MW. Node 0 is set as the balanced node, which is connected to the external power grid. Load nodes 24, 25, 32 are industrial load; load 7, 8, 14, 30, and 31 are commercial load; and load nodes 4, 9, and 26 are selected as controllable nodes. The total dispatch period of ADN is set to one day, and the dispatch interval is 1 h. The predicted data of wind power, PV and load are shown in Figure 4. The parameters of microturbine is from [27]. The electricity purchase prices of ADN from the main network using time-sharing electricity prices and the compensated prices of interruptible load are referred from [28, 29]. The parameters $Pdg_{m1,\min}$, $Qdg_{m1,\min}$, $S_{ij,\min}$ and $P_{k\mathrm{t}\,k,\min}$ are set to zero. And the values of other parameters are provided in Tables 5 and 6.

4.2 | Day-ahead scheduling in ADN system in the base scenario

To verify the performance of the proposed linearised method (CPA), the original problem is formulated directly as the MISCOP model for comparison. In addition, as another commonly utilised linearised method to approximate MISCOP, ε-relaxation method is also included. The results are shown in Table 2.

It shows that the total cost of the MISOCP model is the least, and it contains the least variables and constraints. However, many non-linear constraints are included in the MISOCP model and result in a time-consuming computation. Thus, the MISOCP model should be converted into an MILP model to achieve higher calculation speed. It can be observed that the total costs optimised by the three approaches are close, indicating that the model can still maintain high accuracy after linearisation transformation. Further, compared with ε-relaxation method, the total number of constraints and variables of the CPA are decreased by 12.09%, and 11.88%, respectively. The computing time of the CPA method is reduced by 3.68 s as well, corresponding to a remarkable improvement of efficiency

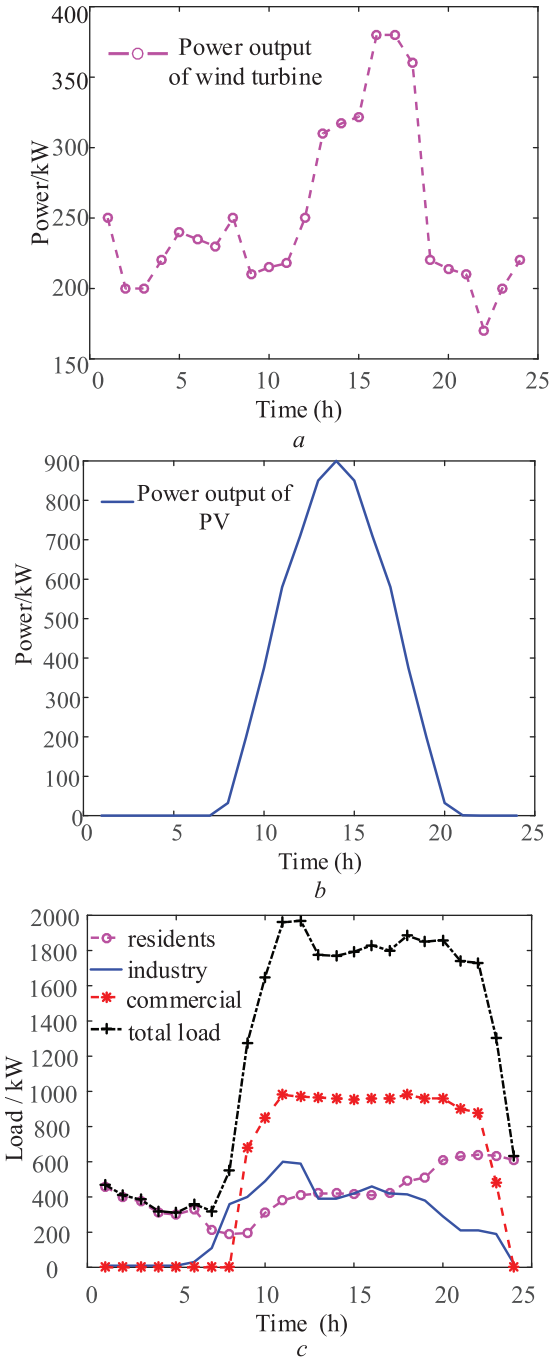

FIGURE 4 The predicted data of wind power, photovoltaic (PV) and load (a) wind, (b) PV, (c) load

by 29.52%. This is because to establish MILP model, the four-dimensional second-order cones constraints as in power flow constraints in Expression (28) are traditionally converted into two three-dimensional second-order cone and linearised by ε-relaxation method with many auxiliary variables and constraints. For the CPA method, the four-dimensional second-order cones can be linearised directly, which need much less auxiliary variables and constraints. Thus, the CPA method in this study has enhanced solution performance.

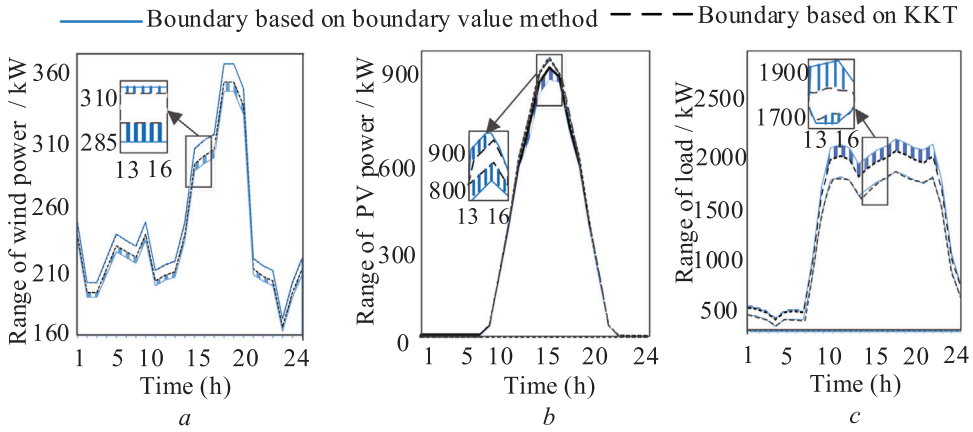

FIGURE 5 Comparing the range of uncertainties based on Karush–Kuhn–Tucker (KKT) conditions and boundary value method (a) wind power, (b) PV power, (c) load

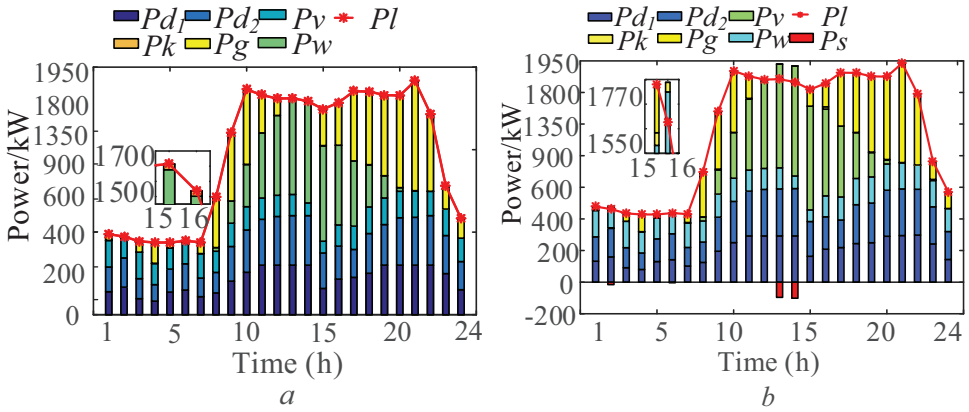

FIGURE 6 The power output of distributed generations, and the sold, purchased and interruptible electricity based on boundary value method and KKT (a) boundary value method, (b) KKT

4.3 | Case studies considering the uncertainties

4.3.1 | Comparing the optimal results based on KKT conditions and boundary value method

The difference between the KKT method and boundary value method [16] in solving multilevel optimisation problems is compared. The fluctuated intervals of wind power, PV and load obtained by KKT conditions and boundary value method are drawn in Figure 5.

The timeslots of enlarged graphics in Figures 5(a)–(c) are all from 1:00 to 4:00 P.M. The range of boundary value method is represented between solid lines, while that of the KKT is reflected between dotted lines. Compared with boundary value method, KKT obtains a smaller range of uncertainties, and the shadow parts in FigureS 5(a)–(c) represent the reduced range of uncertainties. It can be seen that the fluctuated intervals of uncertain parameters are assessed differently through KKT and boundary value method. Then, the minimum and maximum cost are calculated in the obtained intervals by the two methods, respectively. The minimum cost of the two methods are both lower than the expected cost of $9760.69. However, the maximum cost of the boundary value method is higher than the expected cost of $10,159.09, and this verifies that the model based on KKT has a better economic and feasibility. Also, KKT can assess the fluctuated intervals of uncertain horizons more accurately than the boundary value method.

In order to compare the scheduling schemes based on the two methods, the power output of DGs, and the sold, purchased and interruptible electricity are compared in Figure 6.

The enlarged graphics in Figures 6(a) and (b) compare the interrupted loads calculated based on the boundary value method and KKT method from 3:00–4:00 P.M. Figures 6(a) and (b) show that both methods can satisfy power demand.

While scheduling schemes based on the two methods are different since the fluctuation range of wind power, PV, and load are assessed differently. Therefore, the traditional

TABLE 3 The results of three methods

Method	Expected cost/$	Time/s	# of variables
10 scenarios	9978.46	13.394	108,295
Multi-scene [11] 15 scenarios20 scenarios	9971.31	15.898	117,977
	9967.87	17.362	136,769
Robust optimisation [12]	9984.83	8.919	83,405
Improved IGDT	9959.89	8.811	83,341

boundary value method will result in a deviation of the scheduling scheme.

4.3.2 | Comparison of the results among robust optimisation, stochastic optimisation and improved IGDT methods

The Latin hypercube sampling technology with uniform distribution, which only considers the uncertainty of wind power and assumes that the predicted wind power output follows the Gaussian distribution, was used to sample 2000 random wind power output scenarios; and 10, 15, and 20 scenarios are then obtained via scenario reduction. Comparisons among multi-scene optimisation [11], robust optimisation [12], and improved IGDT method are implemented, and the results are listed in Table 3.

Table 3 shows that the results calculated by multi-scene optimisation method are dependent on the number of scenarios. As the number of scenario increases, the randomness of wind power is described more accurately, but it causes more variables and calculation time. And robust scheduling model is to minimise the worst-case cost, which will generate conservative solutions and result in higher expected costs. Compared with these two methods, improved IGDT takes the least computing time and obtains the lowest expected cost of ADN. In addition, another advantage of the proposed improved model in this study that it can assess the fluctuation range of wind power corresponding to the operating cost, which is of great significance to the dispatchers.

4.3.3 | Optimisation results of the ADN model

The uncertainties of wind power, PV and load are obtained by solving the proposed improved model, and it is assumed that $\delta_{cb} = \delta_{co} = \delta$. The results are shown in Table 4.

Table 4 shows that when the deviation factor increases and in order to ensure the economy of system operation, the fluctuation amplitudes of wind power, PV and load also increase. When the deviation factor is set to 0.04, the uncertain values are: $Z_{wa} = 2.36\%$, $Z_{wb} = 6.62\%$, $Z_{va} = 3.31\%$, $Z_{vb} = 3.18\%$, $Z_{la} = 4.76\%$, and $Z_{lb} = 1.14\%$, respectively. This means, when wind power, PV and load fluctuate within [0.9764, 1.0662], [0.9669, 1.0318], and [0.9524, 1.0114] of the predicted value, respectively, the minimum total cost should be lower than $9561.49, and the maximum total cost should be no more than $10,358.29.

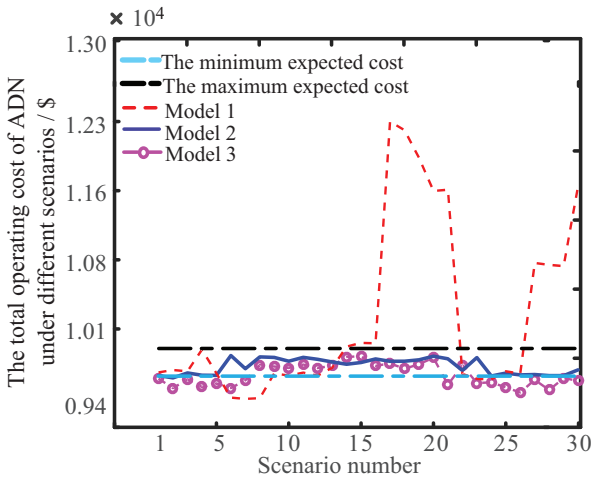

FIGURE 7 The total operating cost of active distribution network under different scenarios of the three models

Similar conclusions are to be expected in the situation of larger distribution networks. The uncertainty of wind power, PV and load make it difficult to be modelled, and the proposed improved IGDT has solved this modelling problem and has been verified in the ADN system. It is essentially the same difficulty to model wind power, PV and load in larger distribution systems for the uncertainties, and so the improved IGDT proposed in this study also applicable to larger distribution systems.

4.3.4 | Comparison of the total cost between the proposed improved and traditional IGDT model

In order to further verify the superiority of the proposed improved model, three models are used to calculate the total cost of day-ahead scheduling in the ADN system.

Model 1: Opportunistic model based on IGDT [14], which tries to guarantee the minimum total cost lower than expected;
Model 2: Robust model based on IGDT [15], which guarantee the maximum total cost lower than expected;
Model 3: The proposed improved model in this study, which tries to guarantee the minimum and maximum total cost lower than expected.

Thirty scenarios of wind power, PV and load are randomly sampled from each uncertainty intervals estimated by three different models based on IGDT. These scenarios are substituted one by one into the deterministic model of ADN, and the calculated total operating costs are shown in Figure 7.

As highlighted in Figure 7, for model 1, it is difficult, under most scenarios, to ensure the total cost of the operation of ADN

TABLE 4 The results of the proposed improved model

δ	Z_{wa}/%	Z_{wb}/%	Z_{va}/%	Z_{vb}/%	Z_{la}/%	Z_{lb}/%
0.00	0.00	0.00	0.00	0.00	0.00	0.00
0.02	1.56	6.02	2.19	2.51	4.16	0.79
0.04	2.36	6.62	3.31	3.18	4.76	1.14
0.06	3.17	7.08	4.46	3.69	5.29	1.61
0.08	3.98	7.55	5.59	4.21	5.88	2.02
0.10	4.78	8.00	6.73	4.70	6.50	2.42
0.12	5.59	8.46	7.86	5.21	7.22	2.83
0.14	6.40	8.88	8.99	5.68	7.97	3.23
0.16	7.20	9.24	10.12	6.08	8.73	3.65

TABLE 5 The values of parameters

Parameter	$V_{i,\min}$	$V_{i,\max}$	$Pdg_{m1,\max}$	$Qdg_{m1,\max}$	$S_{ij,\max}$	$P_{\text{st g,max}}$	$P_{\text{gt g,max}}$
Value	9.5 kV	10.5 kV	300 kW	100 kVar	300 kVA	500 kW	500 kW

to be lower than the minimum expected cost of \$9760.69. Moreover, the total cost of model 1 is high; and for models 3 and 2, the total cost of the operation of ADN under various scenarios can guarantee to be lower than the maximum expected cost \$10,159.09. However, model 3 has a greater possibility of obtaining lower total cost. Consequently, model 3 can secure better economical solution.

5 | CONCLUSION

This study builds an optimal scheduling model of ADN based on the proposed improved IGDT to comprehensively take into account the uncertainties of wind power, PV and load. The original non-linear model is transformed into an SOCP model and then converted to a linear model with a new cone linearisation method based on CPA, which ensures the accuracy and calculation speed of solving the model. The modified IEEE 33-node distribution system is tested to validate the proposed improved model and approach. The main features are summarised as follows.

Considering the uncertainties of wind power, PV and load, a multi-objective optimal scheduling model of ADN is established based on the improved IGDT. This model is successfully used to determine the fluctuation amplitudes of uncertain parameters, and the relationship between the range of uncertain parameters and the lowest acceptable target has been characterised quantitatively so as to provide the decision-making basis for scheduling operators.

The non-linear constraints such as the power flow constraints and branch power limits are transformed into an MILP model with a new cone linearisation method based on CPA. According to the intensive comparisons between the ε-relaxation and the CPA methods, the latter shows a significant advantage in the cone linearisation with fewer requirements of auxiliary variables, distinct improvements on the computational efficiency, and the guarantee of the operating economy.

The proposed improved model is a multilevel optimisation problem and not easy to be solved directly. In this study, KKT conditions are constructed to equivalently convert the original problem into a single-level optimisation problem and enable simultaneous evaluation of maximum and minimum costs. It is verified from the case studies that the model based on KKT is more economic and feasible than that of traditional boundary value method.

In the future work, considering that the energy storage would be an indispensable configuration for wind and PV, various influences of the energy storage on ADN should be investigated. In addition, the uncertainty of different demand-side resources is to be deeply analysed in the optimal operation of ADN.

TABLE 6 The values of of $Pkt\ k$,max

t/h	1	2	3	4	5	6	7	8	9	10	11	12	13	14	15	16	17	18	19	20	21	22	23	24
$P_{kt\ k,\max}$/kW	28	26	26	23	26	27	27	42	61	73	75	72	67	69	73	73	76	74	71	70	72	62	41	34

NOMENCLATURE

Indices

i/j, l, w, v indices of nodes, loads, wind turbines, photovoltaics (PVs)

m_1 indices of DGs (including microturbines, wind turbines, and PV power stations)

t, g, d, k indices of time intervals (in h), feeders, microturbines interruptible loads

Parameters

ΔT length of each time interval (in 1 h)

$S_{ij,max}$ max apparent power on the line between node i and j (in kVA)

Ω_i a collection of nodes connected to node i

B_{ij} electrical susceptance between node i and j

G_{ij} electrical conductance between node i and j

$Pdg_{m_1,\min}$ min active power of the m_1^{th} DG (in kW)

$Pdg_{m_1,\max}$ max active power of the m_1^{th} DG (in kW)

$Qdg_{m_1,\min}$ min reactive power of the m_1^{th} DG (in kVar)

$Qdg_{m_1,\max}$ max reactive power of the m_1^{th} DG (in kVar)

$Pk^t_{k,\min}$, $Pk^t_{k,\max}$ min and max interrupted power of load k at period t (in kW)

$Ps^t_{g,\max}$ max electricity of feeder g sells to the grid at period t (in kW)

$Pg^t_{g,\max}$ max electricity of feeder g purchases from the grid at period t (in kW)

$V_{i,\min}$, $V_{i,\max}$ min and max voltage of node i (in kV)

δ_{cb}, δ_{co} robust and chance profit deviation

$Pd_{d,\min}$, $Pd_{d,\max}$ min and max active power of the microturbine d (in kW)

$Qd_{d,\min}$, $Qd_{d,\max}$ min and max reactive power of the microturbine d (in kVar)

Ck^t_k, Cg^t_g, Cs^t_g compensated prices of responsive load k be reduced, the purchased electricity and sold electricity prices of feeder g at period t (in \$/kWh)

a_d, b_d, c_d scheduling cost coefficient of microturbines

Pwr^t_w, Pvr^t_v, Plr^t_l predicted power of wind turbine w, PV power station v, and load l at period t (in kW)

N_g, N_d, N_k, n number of feeders, microturbines, interruptible loads, and nodes

T time horizon of the problem (in 24 h)

Variables

S^t_{ij} apparent power on the line between node i and j (in kVA)

Pg^t_g purchased electricity of feeder g at period t (in kW)

Ps^t_g electricity sold to the grid of feeder g at period t (in kW)

Pd^t_d power output of the microturbine d (in kW)

$Pdg^t_{m_1}$ power output of the m_1^{th} DG (in kW)

$Qdg^t_{m_1}$ reactive power output of the m_1^{th} DG (in kVar)

Pk^t_k interrupted electricity of load k at period t (in kW)

C_o optimisation total day-ahead cost o

C total day-ahead operation cost of scheduling model (in \$)

V^t_i voltage of node i at period t (in kV)

V^t_j voltage of node j at period t (in kV)

θ^t_{ij} impedance angle of the branch between node i and j at period t

d_1, d_2 binary variables, the value is 0 or 1(if feeder sells electricity to the grid, $d_1 = 1$, $d_2 = 0$; otherwise $d_1 = 0$, $d_2 = 1$).

C_{cb}, C_{co} higher and lower expected cost set by the decision-maker (in \$)

P^t_i, Q^t_i active and reactive power of node i at period t (in kW), (in kVar)

Z_{wa}, Z_{va}, Z_{la} negative deviation rate of wind, PV, and load, and the value range are all in [0,1]

Z_{wb}, Z_{vb}, Z_{lb} positive deviation rate of wind, PV, and load, and the value range are all in [0,1]

Pw^t_w, Pv^t_v, Pl^t_l power output of wind turbine w, PV power station v, and load l at period t (in kW)

Qd^t_d, Qw^t_w, Qv^t_v reactive power output of micro-turbine d, wind turbine w, and PV power station v at period t (in kVar)

ACKNOWLEDGMENT

This work was supported in part by the National Natural Science Foundation of China under Grant 52077130, in part by the Shanghai Engineering Research Center of Green Energy Grid-Connected Technology under Grant 13DZ2251900, in part by the Shanghai Science and Technology Project under Grant 18DZ1203200, and in part by the "Electrical Engineering" Shanghai Class II Plateau Discipline.

ORCID

Xiaohe Zhu https://orcid.org/0000-0001-9984-0461

Yang Mi https://orcid.org/0000-0001-5024-4968

REFERENCES

1. Chen, X., et al.: Optimal control of DERs in ADN under spatial and temporal correlated uncertainties. IEEE Trans. Smart Grid 11(2), 1216–1228 (2020)
2. Liu, B., et al.: A computational attractive interval power flow approach with correlated uncertain power injections. IEEE Trans. Power Syst. 35(1), 825–828 (2020)
3. Nour, A.M.M., et al.: Voltage violation in four-wire distribution networks integrated with rooftop PV systems. IET Renewable Power Gener. 14(13), 2395–2405 (2020)
4. Zhao, T., et al.: A flexible operation of distributed generation in distribution networks with dynamic boundaries. IEEE Trans. Power Syst. 35(5), 4127–4130 (2020)
5. van Ackooij, W., Finardi, E.C., Ramalho, G.M.: An exact solution method for the hydrothermal unit commitment under wind power uncertainty with joint probability constraints. IEEE Trans. Sustainable Energy 33(6), 6487–6500 (2018)
6. Sun, W., et al.: Data-driven probabilistic optimal power flow with nonparametric bayesian modeling and inference. IEEE Trans. Smart Grid 11(2), 1077–1090 (2020)

7. Nazir, F.U., Pal, B.C, Jabr, R.A.: A two-stage chance constrained volt/var control scheme for active distribution networks with nodal power uncertainties. IEEE Trans. Sustainable Energy 34(1), 314–325 (2019)
8. Sadamoto, T., et al.: Spatiotemporally multiresolutional optimization toward supply-demand-storage balancing under pv prediction uncertainty. IEEE Trans. Smart Grid 6(2), 853–865 (2015)
9. Scolari, E., et al.: A comprehensive assessment of the short-term uncertainty of grid-connected PV systems. IEEE Trans. Sustainable Energy 9(3), 1458–1467 (2018)
10. Bo, R., Li, F.: Probabilistic LMP forecasting considering load uncertainty. IEEE Trans. Sustainable Energy 24(3), 1279–1289 (2009)
11. Uçkun, C., Botterud, A., Birge, J.R.: An improved stochastic unit commitment formulation to accommodate wind uncertainty. IEEE Trans. Power Syst. 31(4), 2507–2517 (2016)
12. Chen, X., Wu, W., Zhang, B.: Robust capacity assessment of distributed generation in unbalanced distribution networks incorporating ANM techniques. IEEE Trans. Sustainable Energy 9(2), 651–663 (2018)
13. Ben-Haim, Y.: Information Gap Decision Theory: Designs Under Severe Uncertainty, 2nd edition. Academic Press, San Diego, CA (2006)
14. Dolatabadi, A., Jadidbonab, M., Mohammadi-ivatloo, B.: Short-term scheduling strategy for wind-based energy hub: A hybrid stochastic/IGDT approach. IEEE Trans. Sustainable Energy 10(1), 438–448 (2019)
15. Nikoobakht, A., Aghaei, J.: IGDT-based robust optimal utilisation of wind power generation using coordinated flexibility resources. IET Renewable Power Gener. 11(2), 264–277 (2017)
16. Mohammadi-Ivatloo, B., et al.: Application of information-gap decision theory to risk-constrained self-scheduling of GenCos. IEEE Trans. Power Syst. 28(2), 1093–1102 (2013)
17. Aghaei, J., et al.: Optimal robust unit commitment of CHP plants in electricity markets using information gap decision theory. IEEE Trans. Smart Grid 8(5), 2296–2304 (2017)
18. Guo, Z., et al.: A fast algorithm for optimal power scheduling of large-scale appliances with temporally spatially coupled constraints. IEEE Trans. Smart Grid 11(2), 1136–1146 (2020)
19. Chen, L., Deng, Z., Xu, X.: Two-stage dynamic reactive power dispatch strategy in distribution network considering the reactive power regulation of distributed generations. IEEE Trans. Power Syst. 34(2), 1021–1032 (2019)
20. Tahboub, A.M., et al.: Multiobjective dynamic VAR planning strategy with different shunt compensation technologies. IEEE Trans. Power Syst. 33(3), 2429–2439 (2018)
21. Huang, C., et al.: Second-order cone programming-based optimal control strategy for wind energy conversion systems over complete operating regions. IEEE Trans. Sustainable Energy 6(1), 263–271 (2015)
22. Pareek, P., Verma, A.: Piecewise linearization of quadratic branch flow limits by irregular polygon. IEEE Trans. Power Syst. 33(6), 7301–7304 (2018)
23. Cleave, J.P.: The form of the tangent-developable at points of zero torsion on space curves. Math. Proc. Cambridge Philos. Soc. 88(3), 403–407 (1980)
24. Li, Q., Liu, M., Liu, H.: Piecewise normalized normal constraint method applied to minimization of voltage deviation and active power loss in an AC–DC hybrid power system. IEEE Trans. Power Syst. 30(3), 1243–1251 (2015)
25. Chattopadhyay, D.: Application of general algebraic modeling system to power system optimization. IEEE Trans. Power Syst. 14(1), 15–22 (1999)
26. Jallad, J., et al.: Improved UFLS with consideration of power deficit during shedding process and flexible load selection. IET Renewable Power Gener. 12(5), 565–575 (2018)
27. Heidari, M., et al.: Integrated battery model in cost-effective operation and load management of grid-connected smart nano-grid. IET Renewable Power Gener. 13(7), 1123–1131 (2019)
28. Aalami, H., Yousefi, G.R., Parsa Moghadam, M.: Demand response model considering EDRP and TOU programs. In: 2008 IEEE/PES Transmission and Distribution Conference and Exposition, Chicago, IL, USA, pp. 1–6 (2008)
29. Luo, Y.: Hybrid optimization of system adequacy management in an electricity market. In: 2007 Australasian Universities Power Engineering Conference, Perth, WA, Australia, pp. 1–7 (2007)
30. Ben-Tal, A., Nemirovski, A.: On polyhedral approximations of the second-order cone. Math. Oper. Res. 26(2), 193–205 (2001)

How to cite this article: Ge X., et al.: Optimal day-ahead scheduling for active distribution network based on improved information gap decision theory. *IET Renewable Power Generation*. 2021;15:952–963. https://doi.org/10.1049/rpg2.12045